Site Preference and Si/B Mixing in Mixed-Alkali Borosilicate Glasses: A High-Resolution ^{11}B and ^{17}O NMR Study

Lin-Shu Du* and Jonathan F. Stebbins

Department of Geological and Environmental Sciences, Stanford University, Stanford, California 94305-2115

Received May 29, 2003. Revised Manuscript Received July 21, 2003

In a series of mono and mixed-alkali borosilicate glasses ($\sim 0.7M_2O{\cdot}B_2O_3{\cdot}2SiO_2$, M = Li, Na, K, ($^1/_2Li_2O + \sim^1/_2Na_2O$), ($^1/_2Li_2O + {}^1/_2K_2O$), and ($\sim^1/_2Na_2O + {}^1/_2K_2O$)), we have applied triple-quantum magic-angle spinning (3QMAS) and ^{11}B and ^{17}O NMR to obtain high-resolution information about short-range structure and the connections among various network structural units, to study the effect of mixed cations on the glass structure, and to explore the distribution and mixing of these modifier cations. For a Li-containing glass, a lower fraction of $^{[4]}B$, a lower fraction of Si−O−B, and a higher fraction of nonbridging oxygen than those found in Na- and K-containing glasses suggests that there is a significant heterogeneity in terms of Si/B mixing in the former. For Li−Na and Li−K mixed cation glasses, anomalously high fractions of nonbridging oxygen were also observed along with smaller fractions of $^{[4]}B$ and Si−O−B, again indicating significant chemical heterogeneity. For Na−K mixed cation glasses, the populations of boron and oxygen species are similar to the average population of Na- and K-containing glasses, indicating that these glasses are less heterogeneous. Oxygen-17 and boron-11 chemical shift data indicate cation preferences in coordination by nonbridging oxygen, Si−O−Si, $^{[3]}B$(ring), and $^{[4]}B$ species for Li−Na and Li−K glasses but not for Na−K glass. The result suggests that in the Na−K glass, modifier cations are nearly randomly mixed and the degree of Si/B mixing is similar to that of the Na and K glasses. However, Li−Na and Li−K glasses are likely to contain nanoscale lithium-silicate rich domains embedded in Na/K borosilicate matrixes.

Introduction

Borosilicate glasses are widely applied in many technologies; they are used as optical components, sealing materials, chemically resistant containers, and for the sequestration of radioactive waste.[1] One of the most important properties of these glasses is that phase separation (into silicon-rich and boron-rich phases) occurs in a certain range of compositions,[2,3] which allows the production of porous glasses useful for separation membranes, and enzyme and catalyst supports.[4,5] The degree of mixing among silicon and boron structural species (i.e., Si/B mixing), besides being a critical measure of the tendency to unmix, is also a generally important issue in controlling and designing the physical properties of borosilicate glasses, such as chemical durability, strength at high temperature, and crystal nucleation rates. In commonly used mixed-alkali borosilicate glasses (for example for the vitrification of high-level radioactive waste),[1,6] the extent of network modifier cation mixing may also have an important effect on both viscosity and cation diffusivities, which are key properties in batch processing.[7,8]

Boron-11 NMR has long been one of the major tools for studying the short-range structure of alkali borate and borosilicate glasses. Early work with ^{11}B "wide-line" NMR (low-resolution measurements at low external fields) determined the fraction of tetrahedral (BO_4 groups, denoted here as $^{[4]}B$) and trigonal boron species (BO_3 groups, $^{[3]}B$) including symmetric and asymmetric trigonal boron groups, and led to detailed structural models for sodium borosilicate glasses.[9,10] Quadrupolar coupling constants (C_Q) and asymmetry parameters (η) were also determined for these types of borate groups. C_Q is the measure of the deviation from tetrahedral or higher symmetry of the local bonding environment and η measures the deviation from local cylindrical symmetry.

(1) Deeg, E. W. Industrial borate glasses. In *Borate Glasses: Structure, Properties, and Applications*; Pye, L. D., Frechette, V. D., Kreidl, N. J., Eds.; Plenum: New York, 1978; pp 587−596.
(2) Haller, W.; Blackburn, D. H.; Wagstaff, F. E.; Charles, R. J. *J. Am. Ceram. Soc.* **1970**, *53*, 34−39.
(3) Sastry, B. S. R.; Hummel, F. A. *J. Am. Ceram. Soc.* **1960**, *43*, 23−33.
(4) Yazawa, T. *Key Eng. Mater.* **1996**, *15*, 125.
(5) Yazawa, T. *Porous Ceram. Mater.* **1996**, *115*, 125−146.
(6) Roderick, J. M.; Holland, D.; Scales, C. R. *Phys. Chem. Glasses* **2000**, *41*, 392−395.
(7) Richet, P.; Neuville, D. R. Thermodynamics of silicate melts: configurational properties. In *Thermodynamic Data*; Saxena, S. K., Ed.; Springer-Verlag: New York, 1992; pp 132−161.
(8) Richet, P.; Bouhifd, M. A.; Courtial, P.; Téqui, C. *J. Non-Cryst. Solids* **1997**, *211*, 271−280.
(9) Dell, W. J.; Bray, P. J.; Xiao, S. Z. *J. Non-Cryst. Solids* **1983**, *58*, 1−16.
(10) Yun, Y. H.; Bray, P. J. *J. Non-Cryst. Solids* **1978**, *27*, 363−380.

10.1021/cm034427r CCC: $25.00 © 2003 American Chemical Society
Published on Web 09/04/2003

High-resolution magic angle spinning (MAS) ^{11}B NMR at magnetic field strengths of 11.7 T or above can also provide accurate relative concentrations of trigonal and tetrahedral boron species and estimate quadrupolar parameters.[11−15] More importantly, isotropic chemical shifts (δ_{iso}) can be extracted from MAS NMR, providing additional structural insights when correlated with structure variables such as coordination number, bond distance and angle, and first and second neighbor populations.[11]

Newer techniques such as dynamic angle spinning (DAS)[16] and triple quantum magic angle spinning (3QMAS)[17,18] have been developed to eliminate the second-order quadrupolar broadening, which usually degrades the resolution of MAS spectra of quadrupolar nuclides, by providing two-dimensional (2-D) spectra with one dimension free of such broadening. Boron-11 DAS NMR has resolved and quantified $^{[3]}$B in rings of three BO_3 groups ("boroxol" rings) and nonring $^{[3]}$B in B_2O_3 and alkali borate glasses.[19−23] We have shown recently that even better resolution of such sites can be obtained with ^{11}B 3QMAS, particularly at relatively high magnetic fields such as 14.1 T.[13,24−26]

Oxygen-17 NMR can provide information about connectivities among various cations, about network bond angles, and about cation order/disorder in borosilicates. The greatly improved resolution provided by ^{17}O 3QMAS has allowed resolution of various types of bridging oxygen sites such as Si−O−Si, Si−O−B, and B−O−B as well as nonbridging oxygens (NBOs).[24,27−29]

In our recent NMR study of alkali borosilicate glasses,[24,30] we showed that even more detailed structural units can be found in 3QMAS spectra, including $^{[3]}$B(ring), $^{[3]}$(nonring), $^{[4]}$B(iB,(4-i)Si) for i = 0, 1, 2 in ^{11}B data, and NBO, Si−O−Si, Si−O−$^{[4]}$B, Si−O−$^{[3]}$B, $^{[4]}$B−O−$^{[3]}$B, and $^{[3]}$B−O−$^{[3]}$B in ^{17}O data. This provides a greatly increased amount of information to explore issues such as the effects of alkali type and content, of Si/B ratio, and of annealing on the glass structure. Furthermore, the mean number of Si coordinated to boron units can be obtained by combination of ^{17}O and ^{11}B NMR data.

The "mixed-alkali effect" is a long-studied and intriguing property of complex glasses.[31−33] The effect is characterized by large deviations from linearity with composition (ratio of two alkalis) in physical parameters, particularly transport properties such as electrical conductivity and viscosity. Various models have been proposed to explain this behavior in terms of the spatial distribution of the cations. For example, the modifier cations could undergo homogeneous distribution or clustering, with either random or nonrandom mixing.[34−38]

The spin−echo double resonance NMR technique (SEDOR) has been applied in studying the distribution and mixing of the modifier cations in mixed-alkali silicates (Li−Na) and borates (Li−Na, Li−K).[35,38−42] The first ^{23}Na{^{7}Li} SEDOR study on Li−Na silicate glasses along with molecular dynamics calculations suggested like-cation clustering.[38] However, later ^{23}Na{^{7}Li} and ^{23}Na{^{6}Li} results indicated that these cations are randomly mixed and homogeneously distributed in the glass network.[35,39−42]

The addition of modifier oxides to silicate glasses, and to borate and borosilicate glasses in certain composition ranges, generates nonbridging oxygens (NBOs). Oxygen-17 NMR is therefore an ideal tool to probe the mixing of the cations associated with NBO. Oxygen-17 MAS, DAS, and 3QMAS NMR techniques have been applied to Ca−Mg,[43,44] K−Mg,[44,45] Na−K,[46] Ca−Ba,[47] and Na−Ca[48] silicate glasses. Random mixing was suggested in Ca−Ba, Ca−Mg, and Na−K silicate glasses, but clearly nonrandom distributions were found in the Na−Ca and K−Mg systems.

(11) Kroeker, S.; Stebbins, J. F. *Inorg. Chem.* **2001**, *40*, 6239−6246.
(12) Schramm, S.; Oldfield, E. *J. Chem. Soc., Chem. Commun.* **1982**, 980−981.
(13) Sen, S.; Xu, Z.; Stebbins, J. F. *J. Non-Cryst. Solids* **1998**, *226*, 29−40.
(14) Turner, G. L.; Smith, K. A.; Kirkpatrick, R. J.; Oldfield, E. *J. Magn. Reson.* **1986**, *67*, 544−550.
(15) Turner, G. L.; Kirkpatrick, R. J.; Risbud, S. H.; Olfield, E. *Am. Ceram. Soc. Bull.* **1987**, *66*, 656−663.
(16) Mueller, K. T.; Sun, B. Q.; Chingas, G. C.; Zwanziger, J. W.; Terao, T.; Pines, A. *J. Magn. Reson.* **1990**, *86*, 470−487.
(17) Frydman, L.; Harwood: J. S. *J. Am. Chem. Soc.* **1995**, *117*, 5367−5368.
(18) Medek, A.; Harwood: J. S.; Frydman, L. *J. Am. Chem. Soc.* **1995**, *117*, 12779.
(19) Youngman, R. E.; Zwanziger, J. W. *J. Non-Cryst. Solids* **1994**, *168*, 293−297.
(20) Youngman, R. E.; Haubrich, S. T.; Zwanziger, J. W.; Janicke, M. T.; Chmelka, B. F. *Science* **1995**, *269*, 1416−1420.
(21) Youngman, R. E.; Zwanziger, J. W. *J. Am. Chem. Soc.* **1995**, *117*, 1397−1402.
(22) Youngman, R. E.; Zwanziger, J. W. *J. Phys. Chem.* **1996**, *100*, 16720−16728.
(23) Zwanziger, J. W.; Youngman, R. E.; Braun, M. High-resolution NMR studies of borate glass structure. In *Borate Glasses, Crystals and Melts*; Wright, A. C., Feller, S. A., Hannon, A. C., Eds.; Society of Glass Technology: Sheffield, UK, 1997; pp 21−32.
(24) Du, L.-S.; Stebbins, J. F. *J. Non-Cryst. Solids* **2003**, *315*, 239−255.
(25) Lee, S. K.; Musgrave, C. B.; Zhao, P.; Stebbins, J. F. *J. Phys. Chem. B* **2001**, *105*, 12583−12595.
(26) Lee, S. K.; Stebbins, J. F. *Geochim. Cosmochim. Acta* **2002**, *66*, 303−309.
(27) Wang, S.; Stebbins, J. F. *J. Non-Cryst. Solids* **1998**, *231*, 286−290.
(28) Wang, S.; Stebbins, J. F. *J. Am. Ceram. Soc.* **1999**, *82*, 1519−1528.
(29) Zhao, P.; Kroeker, S.; Stebbins, J. F. *J. Non-Cryst. Solids* **2000**, *276*, 122−131.
(30) Du, L.-S.; Stebbins, J. F. *J. Phys. Chem. B* **2003**, in press.
(31) Isard, J. O. *J. Non-Cryst. Solids* **1969**, *1*, 235.
(32) Day, D. E. *J. Non-Cryst. Solids* **1976**, *21*, 343.
(33) Ingram, M. D. *Phys. Chem. Glasses* **1987**, *28*, 215−234.
(34) Bray, P. J.; Emerson, J. F.; Lee, D.; Feller, S. A.; Brain, D. L.; Feil, D. A. *J. Non-Cryst. Solids* **1991**, *129*, 240−248.
(35) Gee, B.; Eckert, H. *J. Phys. Chem.* **1996**, *100*, 3705−3712.
(36) Greaves, G. N. *J. Non-Cryst. Solids* **1985**, *71*, 203-217.
(37) Ingram, M. D. *J. Am. Ceram. Soc.* **1980**, *63*, 248.
(38) Yap, A. T.-W.; Förster, H.; Elliott, S. R. *Phys. Rev. Lett.* **1995**, *75*, 3946−3949.
(39) Gee, B.; Eckert, H. *Ber. Bunsen-Gesell. Phys. Chem.* **1996**, *100*, 1610−1616.
(40) Gee, B.; Janssen, M.; Eckert, H. *J. Non-Cryst. Solids* **1997**, *215*, 41−50.
(41) Ratai, E.; Janssen, M.; Eckert, H. *Solid State Ionics* **1998**, *105*, 25−37.
(42) Ratai, E.; Chan, J. C. C.; Eckert, H. *Phys. Chem. Chem. Phys.* **2002**, *4*, 3198−3208.
(43) Kirkpatrick, R. J. MAS NMR spectroscopy of minerals and glasses. In *Spectroscopic Methods in Mineralogy and Geology*; Hawthorne, F. C., Ed.; Mineralogical Society of America: Washington DC, 1988; pp 341−403.
(44) Allwardt, J. R.; Stebbins, J. F. *Am. Mineral*, submitted for publication.
(45) Farnan, I.; Grandinetti, P. J.; Baltisberger, J. H.; Stebbins, J. F.; Werner, U.; Eastman, M.; Pines, A. *Nature* **1992**, *358*, 31−35.
(46) Florian, P.; Vermillion, K. E.; Grandinetti, P. J.; Farnan, I.; Stebbins, J. F. *J. Am. Chem. Soc.* **1996**, *118*, 3493−3497.
(47) Stebbins, J. F.; Oglesby, J. V.; Xu, Z. *Am. Mineral.* **1997**, *82*, 1116−1124.
(48) Lee, S. K.; Stebbins, J. F. *J. Phys. Chem. B* **2003**, *107*, 3141−3148.

Table 1. Sample Names and Nominal Compositions

	mole fraction (0.002)				
sample name	Li_2O	Na_2O	K_2O	B_2O_3	SiO_2
LBS	0.200			0.267	0.533
NBS		0.175		0.275	0.550
KBS			0.200	0.267	0.533
LN−BS	0.102	0.086		0.271	0.541
LK−BS	0.100		0.143	0.267	0.533
NK−BS		0.086	0.102	0.271	0.541

In our preliminary study of mixed-alkali borosilicate glasses presented here, three optically clear mixed-alkali (Li−Na, Li−K, Na−K) borosilicate glasses with the same Si/B ratio and similar modifier cation ratios were made and examined by ^{11}B and ^{17}O NMR. Oxygen-17 3QMAS NMR clearly demonstrates the effects of mixed cations on Si/B mixing. The varying effects of different modifier cations on ^{11}B and ^{17}O chemical shifts of each structural unit[24] also provide considerable information on distributions of modifier cations and the extent of their mixing.

Experimental Section

Sample Preparation. Samples were synthesized from dried Li_2CO_3, Na_2CO_3, K_2CO_3, B_2O_3, and ^{17}O-enriched SiO_2. Nominal compositions are represented in this paper by *K* and *R* values defined as the molar ratio of SiO_2 to B_2O_3 and Na_2O to B_2O_3, respectively. Sample names and nominal compositions are given in Table 1. To speed spin−lattice relaxation and allow more rapid NMR data collection, about 0.2 wt % Co_3O_4 was added to each 300-mg sample. Oxygen-17 enriched silica was prepared by hydrolyzing silicon tetrachloride with 47% ^{17}O-enriched water in a diethyl ether solvent, followed by dehydration at high temperature in Ar. The starting materials were mixed thoroughly, then heated in platinum crucibles in Ar first at 600 °C to allow decarbonation and then at 1100 °C for 30 to 80 min. Each sample was quenched by dipping the bottom of the crucible in cold water. All resulting glasses were found to be optically homogeneous on examination at 400× with an optical microscope.

NMR Data Collection. NMR spectra were collected on a Varian Unity/INOVA 600 spectrometer (14.1 T) at 81.3 and 192.4 MHz for ^{17}O and ^{11}B, respectively. Oxygen-17 and boron-11 chemical shifts are expressed in parts per million (ppm) relative to ^{17}O-enriched H_2O at 0 ppm and 1.0 M boric acid at 19.6 ppm, respectively. A Varian/Chemagnetics T3-DR probe with 3.2-mm ZrO_2 rotors and spinning speeds of 20 kHz was used. The ^{11}B MAS spectra were obtained using a single hard pulse, with radio frequency (rf) powers of 115 kHz. To obtain more quantitative spectra, an rf tip angle of less than one-third of the solid 90° pulse duration was employed, resulting in 0.3-μs long pulses for single-pulse experiments. Relaxation delays of 5 s were used for ^{11}B MAS experiments. Both ^{17}O and ^{11}B 3QMAS spectra were acquired using a shifted-echo pulse sequence.[49] For ^{17}O 3QMAS experiments, the optimized lengths of the triple quantum excitation and reconversion pulses were about 3.0 and 1.0 μs, with an rf power of 150 kHz. A soft 180° pulse, selecting the central transition only, immediately after an echo time of 1 ms, was set to 24 μs at an rf power of 9 kHz. About 80−120 t_1 with 96−192 FIDs per t_1 point were collected with a delay of 8−10 s. For the ^{11}B 3QMAS experiments, the optimized lengths of first and second pulses with an rf power of 170 kHz were about 3.6 and 1.1 μs. The length of the third pulse was about 34 μs with an rf power of 10 kHz after an echo time of 3 ms. About 240 t_1 with 48−96 FIDs per t_1 point were collected with a delay of 8−10 s. All 3QMAS data were processed using the RMN program (P. J. Grandinetti, Ohio State University), including a shear transformation.

Central transition line shapes of the ^{11}B MAS spectra were simulated with the program Wsolid (R. E. Wasylishen and K. E. Eichele, Dalhousie University, 1999) with an approximation of infinite spinning speed. Initial constraints on isotropic δ_{iso}, quadrupolar C_Q, and η for each boron site were taken from the quadrupolar coupling parameter P_Q ($= C_Q(1 + \eta^2/3)^{1/2}$) and δ_{iso} obtained from the centers of gravity of the peaks in the two dimensions of the ^{11}B 3QMAS spectra as previously described.[18,50,51] Estimates of δ_{iso} and P_Q for oxygen sites were derived in a similar manner from the ^{17}O 3QMAS spectra with no attempt at fitting the unresolved MAS spectra.

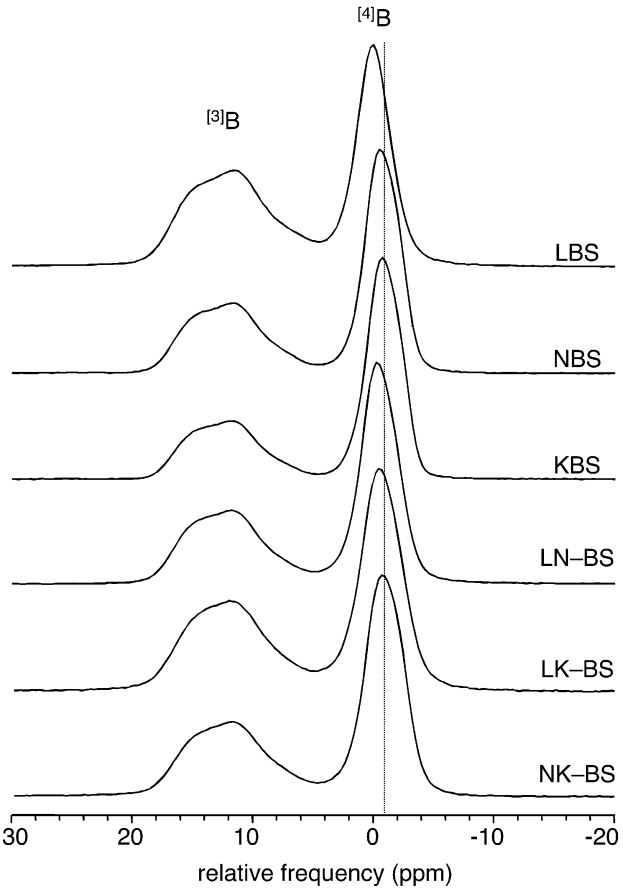

Figure 1. Boron-11 MAS spectra for LBS, NBS, KBS, LN−BS, LK−BS, and NK−BS glasses. The vertical dotted line highlights small changes in the $^{[4]}B$ chemical shift. Here, and in the following figures, the intensity of each spectrum is normalized to that of its highest peak.

Results

Boron-11 NMR. The ^{11}B MAS spectra of the glasses are shown in Figure 1. Signals from $^{[3]}B$ and $^{[4]}B$ groups (centered around 12 and 0 ppm, respectively) are very well resolved at this field (14.1 T) as been recently noted,[13,24] and therefore the relative intensities of the two types of sites can be easily determined by integration.

As was described in our previous paper,[24] more detailed boron structural units can be resolved with ^{11}B 3QMAS. This technique produces two-dimensional

(49) Massiot, D.; Touzo, B.; Trumeau, D.; Coutures, J. P.; Virlet, J.; Florian, P.; Grandinetti, P. J. *Solid State NMR* **1996**, *6*, 73−83.

(50) Baltisberger, J. H.; Xu, Z.; Stebbins, J. F.; Wang, S. H.; Pines, A. *J. Am. Chem. Soc.* **1996**, *118*, 7209−7214.

(51) Schaller, T.; Stebbins, J. F. *J. Phys. Chem. B* **1998**, *102*, 10690−10697.

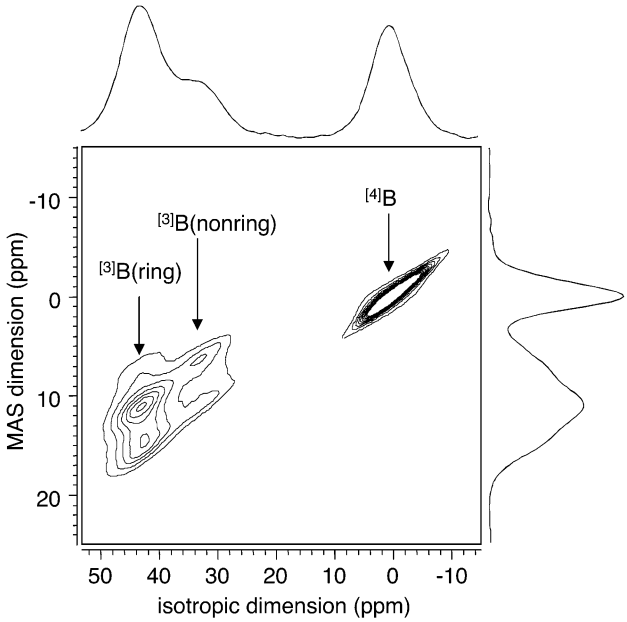

Figure 2. Contour plot of the ^{11}B 3QMAS spectrum for LBS glass. The spectra projected (summed) along both dimensions are also displayed adjacent to the axes.

(2-D) spectra generally displayed as contour plots. One dimension retains the second-order quadrupolar broadening and is equivalent to a somewhat distorted version of the MAS spectrum; the other (isotropic) dimension is free of second-order quadrupolar broadening, often providing much higher resolution.[17,18,49] In the ^{11}B 3QMAS spectrum for a lithium borosilicate glass (NBS−K2R0.75), at least three peaks are partially resolved (Figure 2). Two [3]B peaks having significant broadening in the MAS dimension, along with a less broadened [4]B peak, are centered at about 43, 33, and 2 ppm, respectively, in the isotropic dimension. In the isotropic-dimension projections, it is easier to observe the changes in shift and intensities with composition, which reflect the changes in environments and populations of boron species (Figure 3). Two roughly Gaussian components for [3]B and at least two for [4]B are observed, distinguished primarily by chemical shift differences that become particularly noticeable at the high external magnetic field employed here. On the basis of recent high-resolution ^{11}B NMR studies,[11,19−22,24,26,52] the two components of the [3]B NMR peak can be attributed to boron in boroxol rings and to [3]B in nonring sites. As previously determined, the unresolved [4]B component peaks were assigned as [4]B(2B,2Si), [4]B(1B,3Si), and [4]B(0B,4Si), respectively. This was based on the detailed comparison between the chemical shifts of these peaks and the known boron species in crystalline materials as well as the relationship between the evolution of the peak shapes and the changes of boron species with Si/B ratio.[24,30]

To obtain the populations of each B species, δ_{iso} and P_Q were first estimated from the centers of gravity in the 2-D spectra as described in the Experimental Section, and slices through the peaks in the 2-D spectra along the MAS dimension were fit to estimate the η values. These results were then used as starting points

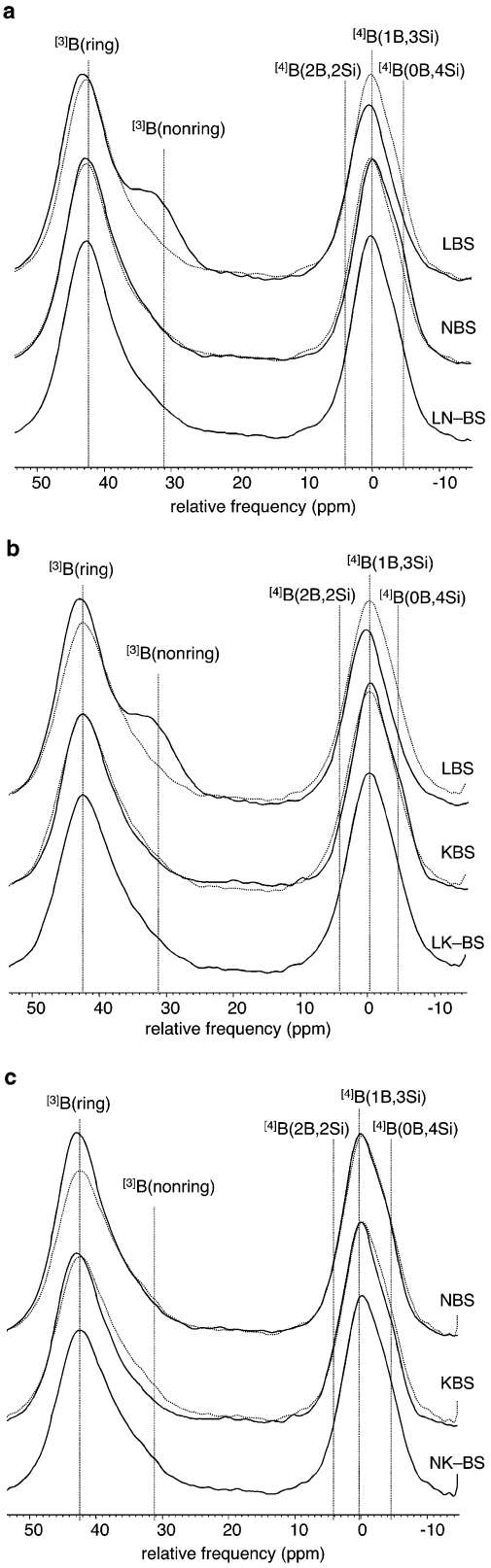

Figure 3. Isotropic projections of ^{11}B 3QMAS spectra for (a) LN−BS compared with LBS and NBS, (b) LK−BS compared with LBS and KBS, (c) NK−BS compared with NBS and KBS. In each plot, the spectrum for the mixed alkali glass is overlayed as a dotted line to allow detailed comparison. Vertical dotted lines are guides indicating the approximate positions of the peaks for [3]B(ring), [3]B(nonring), [4]B(2B,2Si), [4]B(1B,3Si), and [4]B(0B,4Si).

(52) Youngman, R. E.; Werner-Zwanziger, U.; Zwanziger, J. W. *Z. Naturforsch.* **1996**, *51*, 321−329.

Table 2. Fraction of Boron Species Obtained from the Simulation of ^{11}B MAS Spectra in Figure 1

sample name	$^{[3]}$B(ring)	$^{[3]}$B(nonring)	$^{[4]}$B(2B,2Si)	$^{[4]}$B(1B,3Si)	$^{[4]}$B(0B,4Si)	$^{[3]}$B	$^{[4]}$B
LBS	0.371(2)	0.178(2)	0.053(5)	0.313(5)	0.084(5)	0.550(2)	0.450(2)
NBS	0.306(2)	0.128(2)	0.052(5)	0.326(5)	0.189(5)	0.433(2)	0.567(2)
KBS	0.313(2)	0.088(2)	0.039(5)	0.351(5)	0.210(5)	0.400(2)	0.600(2)
LN−BS	0.337(2)	0.111(2)	0.048(5)	0.323(5)	0.181(5)	0.448(2)	0.552(2)
LK−BS	0.336(2)	0.141(2)	0.033(5)	0.297(5)	0.193(5)	0.477(2)	0.523(2)
NK−BS	0.314(2)	0.130(2)	0.040(5)	0.287(5)	0.230(5)	0.443(2)	0.557(2)

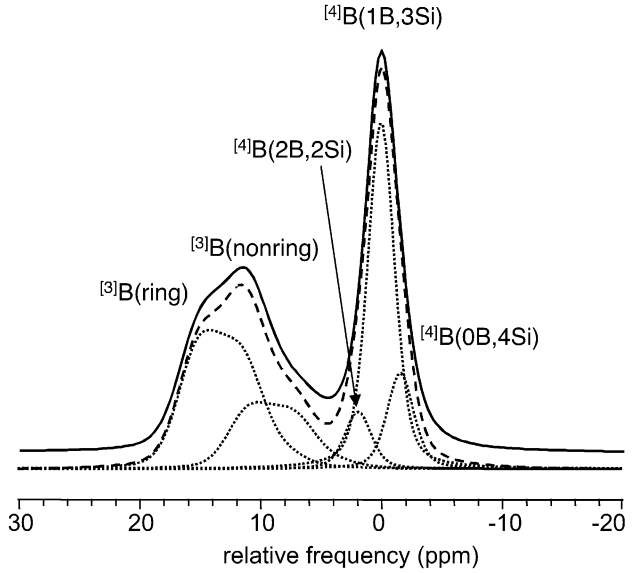

Figure 4. Typical experimental ^{11}B MAS NMR spectrum (solid line) and fitting results (dashed line, sum; dotted lines, components) for LBS glass. Fit parameters are given in Table 2.

for fits of the MAS spectra based on a five-species model (two $^{[3]}$B and three $^{[4]}$B site types). Mixed Gaussian−Lorentzian line broadening was applied to calculate the line shapes, possibly broadened by the distributions of chemical shift and quadrupolar parameters and residual dipolar couplings, in the $^{[3]}$B and $^{[4]}$B regions independently. Note that broadening parameters are the same for components in the same region. A stronger constraint on chemical shift is necessary in order to fit the unresolved peaks in the $^{[4]}$B region by three components. Our previous thorough NMR study on sodium borosilicate glasses shows that the separation in chemical shift between $^{[4]}$B(2B,2Si), $^{[4]}$B(1B,3Si), and $^{[4]}$B(0B,4Si) is about 1.8 ppm,[30] which is the major constraint for the fitting of peaks in the $^{[4]}$B region. In this case, the relative intensities were the only unconstrained parameters in the curve fitting process. The systematic difference between the intensities for the $^{[3]}$B and $^{[4]}$B species caused by their very different C_Q and η values was taken into account when estimating their relative populations from the peak areas in center bands.[53] Results are tabulated in Table 2, and Figure 4 shows an example of a fully simulated spectrum.

Oxygen-17 NMR. As we showed previously for borate and borosilicate glasses,[24,26−29,54] resolution in conventional ^{17}O MAS spectra is poor, but 3QMAS can provide much better resolution for structure analysis (Figure 5). At least four peaks are partially resolved in the 2-D plots. These peaks can be assigned to bridging oxygens (BOs), Si−O−Si, Si−O−B, and B−O−B, and nonbridging oxygen (NBO), based on our previous studies of glasses and crystalline model compounds.[24,26−30,54] It is apparent that the position of the NBO peak in the 2-D spectra varies considerably with the different modifier cations. This can provide information regarding the preference of these ions to associate with NBO, as will be discussed below.

The isotropic projections of the ^{17}O 3QMAS spectra of the mixed-alkali glasses are compared with those of related mono-alkali glasses in Figure 6. For each mixed pair, the average of the spectra of the corresponding two mono-alkali glasses is also shown. The three main peaks that originate from the three types of bridging oxygens, and their positions and relative intensities, vary considerably with the identity of the modifier cations. Our previous studies have shown that peaks associated with Si−O−B and B−O−B are composed of $^{[4]}$B−O−Si, $^{[3]}$B−O−Si, $^{[4]}$B−O−$^{[3]}$B, and $^{[3]}$B−O−$^{[3]}$B, based on the changes in the populations of these species with respect to the change in the $^{[4]}$B/$^{[3]}$B ratio with varying R and an assumption that the energetically less favorable $^{[4]}$B−O−$^{[4]}$B has an insignificant concentration in these compositions ("$^{[4]}$B avoidance").[24]

Simulation of the ^{17}O MAS spectra for these glasses is difficult due to their breadths and lack of significant discontinuities or other characteristic features. However, the isotropic projections of the 3QMAS spectra can each be fit with at least five Gaussian peaks (Figure 7), yielding relative intensities and δ_{iso} and P_Q values. The relative intensities obtained from 3QMAS spectra may need to be calibrated because of the difference in excitation and reconversion efficiencies for oxygen sites with different C_Q values. In a previous ^{17}O 3QMAS study of aluminosilicate glasses, a simple approximation of the reduction of 3QMAS efficiency versus C_Q was proposed using a Gaussian function involving C_Q and δ, a parameter that varies with the experimental conditions.[55] The same approach was applied with the current experimental conditions (higher external field and rf power) and the result shows that the relative intensity obtained directly from the ^{17}O isotropic projection is within a 5% error with C_Q varying from 4.8 to 5.5 MHz, which is the range of C_Q for each type of bridging oxygen in ternary borosilicate glasses.[24,30] Therefore, corrections for the effects of excitation and reconversion efficiencies for bridging oxygens are minor, and have not been applied. The fitted areas are thus good first approximations of the proportions of different sites (Table 3). Note that P_Q for nonbridging oxygens connected to Si is about 2 MHz, and the relative 3QMAS peak intensity may thus be somewhat greater than the

(53) Massiot, D.; Bessada, C.; Coutures, J. P.; Taulelle, F. *J. Magn. Reson.* **1990**, *90*, 231−242.

(54) Stebbins, J. F.; Zhao, P.; Lee, S. K.; Oglesby, J. V. *J. Non-Cryst. Solids* **2001**, *293−295*, 67−73.

(55) Lee, S. K.; Stebbins, J. F. *J. Phys. Chem. B* **2000**, *104*, 4091−4100.

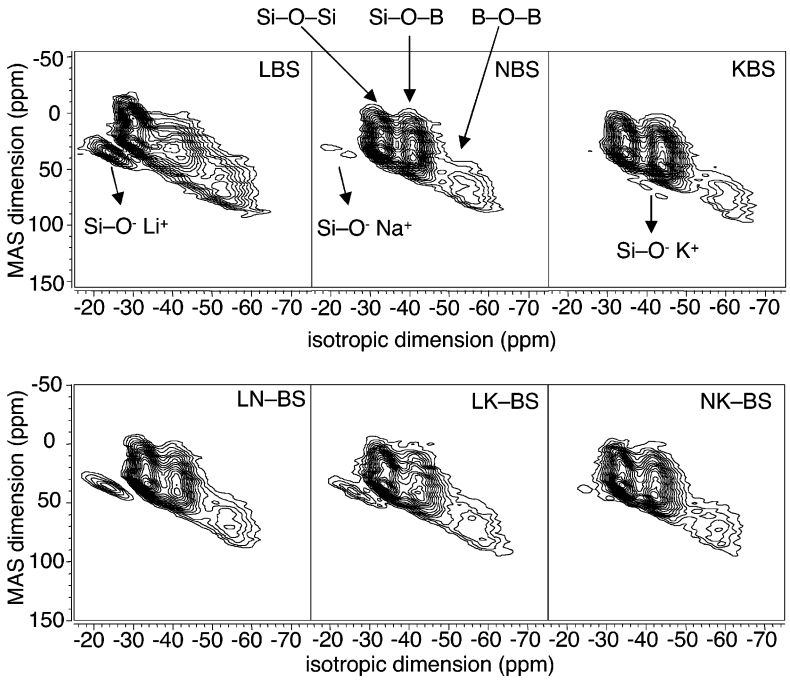

Figure 5. Contour plots of ^{17}O 3QMAS spectra for LBS, NBS, KBS, LN−BS, LK−BS, and NK−BS glasses.

Table 3. Fraction of Oxygen Species for Bridging Oxygens Obtained from the Line fitting of the isotropic projections in ^{17}O 3QMAS Data

sample name	Si−O−$^{[4]}$B	Si−O−$^{[3]}$B	$^{[4]}$B−O−$^{[3]}$B	$^{[3]}$B−O−$^{[3]}$B	Si−O−Si	Si−O−B	B−O−B
LBS	0.153(5)	0.240(5)	0.145(5)	0.105(5)	0.287(5)	0.393(5)	0.250(5)
NBS	0.384(5)	0.082(5)	0.094(5)	0.086(5)	0.332(2)	0.466(5)	0.180(5)
KBS	0.359(5)	0.166(5)	0.079(5)	0.053(5)	0.327(5)	0.524(5)	0.132(5)
LN−BS	0.334(5)	0.099(5)	0.123(5)	0.061(5)	0.322(2)	0.433(5)	0.184(5)
LK−BS	0.265(5)	0.139(5)	0.111(5)	0.064(5)	0.363(5)	0.404(5)	0.175(5)
NK−BS	0.291(5)	0.169(5)	0.110(5)	0.064(5)	0.339(2)	0.460(5)	0.174(5)

Table 4. Information of NBO Including δ_{iso} and P_Q Obtained From ^{17}O 3QMAS Data and Fractions of NBO Obtained via Integration in ^{17}O 2-D Spectra, Curve Fitting from ^{17}O Isotropic Projection, Derivation from N_4, and Prediction from Dell and Bray Model

sample name	δ_{iso}(NBO) ppm (0.2)	P_Q MHz (0.05)	fraction of NBO from ^{17}O spectra: line fitting (0.005)	fraction of NBO from ^{17}O spectra: integration (0.005)	fraction of NBO calculated from N_4 (from ^{11}B spectra) (0.002)	fraction of NBO calculated from Dell and Bray model (0.002)
LBS	41.6	2.34	0.070	0.074	0.077	0.032
NBS	38.0	2.05	0.022	0.027	0.018	0.003
KBS	71.3	1.95	n.a.	0.017[a]	0.039	0.032
LN−BS	39.6	2.29	0.060	0.057	0.037	0.018
LK−BS	43.4	2.26	0.058	0.056	0.059	0.032
NK−BS	48.0	2.47	0.027	0.018[a]	0.035	0.018

[a] The integration may be underestimated due to a slight overlap between BO and NBO.

true NBO population, although our recent ^{17}O 3QMAS study of barium borosilicate glasses at the same magnetic and rf fields yielded surprisingly good agreement between NBO fractions derived from ^{17}O 3QMAS and ^{11}B MAS data.[29] Comparison of the fractions of NBO obtained from ^{17}O 3QMAS and those obtained from ^{11}B NMR will be further addressed in the discussion.

Because the peak position of NBO of the potassium-containing glass is superimposed with the peak positions of the bridging oxygens in the isotropic projection, the relative intensity of NBO for this sample can be obtained only by the integration of NBO in the 2-D spectrum. The obtained value could thus be somewhat underestimated because the NBO peak is also slightly overlapped with bridging oxygens in the 2-D spectrum. The relative intensities of the bridging oxygens were then obtained via curve fitting of the isotropic projection without considering the small contribution of NBO (<2%) to its area.

Discussion

Fractions of NBO. Two approaches to estimating the fraction of NBO from the 3QMAS spectra were taken: by curve fitting of the isotropic projections and by directly integrating the 2-D spectra (Table 4). Curve fitting of the KBS data was not possible because the NBO peak is superimposed on the BO region in the isotropic projection. Both approaches generally show similar results, indicating that these values are reliable. One exception seems to be NK−BS, where the NBO peak is also slightly overlapped with the BO peaks in 2-D spectra, which results in a low value. These estimations are based on the assumption that the excitation and reconversion efficiencies of the 3QMAS pulse se-

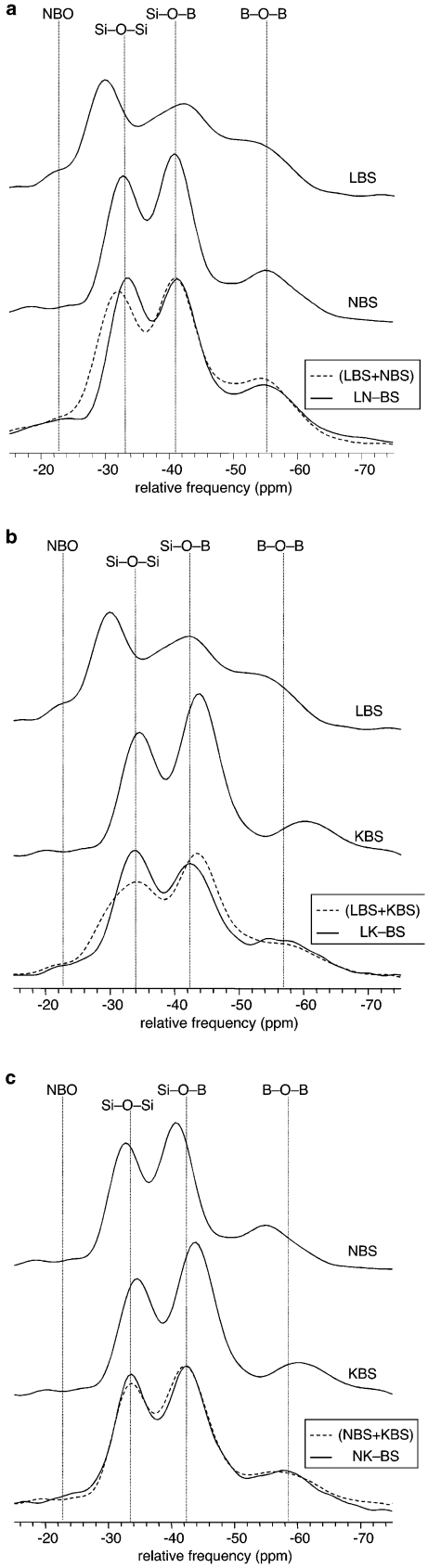

Figure 6. Isotropic projections of ^{17}O 3QMAS spectra for (a) LN−BS, (b) LK−BS, and (c) NK−BS, each compared to the appropriate mono-alkali samples. In each case, the average of the two mono-alkali glasses is shown by a dashed line for comparison. The vertical dotted lines are guides indicating the approximate positions of the peaks as labeled.

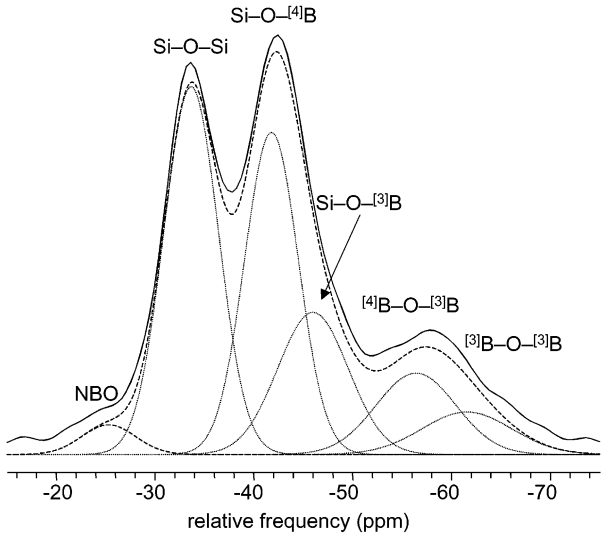

Figure 7. Experimental ^{17}O isotropic projection (solid line) and typical fitting results (dashed line, sum; dotted lines, components) for NK−BS glass. Fit parameters are given in Table 3.

quence are the same for each oxygen species. Fortunately, this can be tested by an independent measure of the fraction of NBO derived from ^{11}B data.

The addition of modifier oxides generally results in the conversion of $^{[3]}B$ to $^{[4]}B$ and, at higher R, to the formation of NBO.[9,10] For a composition RNa$_2$O·B$_2$O$_3$·KSiO$_2$, the total number of Na, O, and B are $2R$, $(R + 2K + 3)$, and 2, respectively. The total number of $^{[4]}B$ is then $2N_4$, and the fraction of NBO is $2(R - N_4)/(R + 2K + 3)$. With the known R and K and the fraction of $^{[4]}B$ (N_4) obtained from the ^{11}B NMR, the fraction of NBO can then be calculated (Table 4). The fractions of NBO estimated from the ^{17}O data are surprisingly similar to the values derived from ^{11}B data, as was seen previously in a study of barium borosilicate glasses using similar experimental conditions.[29] Note that the significant discrepancy in the fraction of NBO in KBS glass may result from the underestimated value obtained from the integration of the NBO peak, which is slightly overlapped with BO in the 2-D spectrum.

The fraction of NBO can also be calculated directly from the Dell and Bray model, which is based on "wideline" ^{11}B NMR on sodium borosilicates.[9] In this model, when the value of R is above $(0.5 + K/16)$, the addition of further Na$_2$O results in the formation of NBO. The predicted fraction of NBO (Table 4) is therefore $2(R - 0.5 - K/16)/(R + 2K + 3)$. Large discrepancies between the observed and predicted values are seen for the LBS, LN−BS, and LK−BS glasses. A smaller, but still noticeable discrepancy is also seen in the NBS glass. As discussed below, this discrepancy may result from chemical heterogeneity in these compositions.

Chemical Heterogeneity. In our previous study, we proposed that the significant observed differences in oxygen and boron species distributions for LBS compared with those of NBS and KBS glasses were caused by considerable chemical heterogeneity.[24] Unlike NBS and KBS, the composition of LBS ($K = 2$, $R = 0.75$) is located near the center of the immiscibility region in the ternary system.[2,3] It is therefore possible for the glass to be phase separated into boron- and silicon-rich

domains, possibly on a sub-optical length scale, if the quench rate was not fast enough to bring the glass transition temperature above the solvus. If the LBS glass were a homogeneous single phase, the Dell and Bray model would predict that N_4 and the fraction of NBO should be around 0.625 and 0.032, respectively.[9] The smaller observed N_4 value (0.45) and larger fraction of NBO (0.074) may thus be due to chemical heterogeneity. This speculation may be tested by roughly estimating the compositions of the two phases that might form from this sample ($0.75Li_2O{\cdot}B_2O_3{\cdot}2SiO_2$) as $0.45Li_2O{\cdot}B_2O_3{\cdot}0.5SiO_2$ and $0.30Li_2O{\cdot}1.5SiO_2$ (the exact compositions do not matter greatly). Summing the expected structural units in the hypothesized two phase gives $N_4 = 0.45$ and the fraction of NBO = 0.077, which are close to our experimental findings. Phase separation may also explain the considerably larger fraction of $^{[3]}$B(nonring) in LBS glass (Figure 3), as our previous study showed this species increases as R decreases in sodium borosilicate glasses.[24]

The differences in the fractions of NBO between experiment and the Dell and Bray model can thus be an indication of the homogeneity of alkali borosilicate glasses. For example, the very small deviation for KBS glass indicates that a homogeneous phase was formed, whereas a slightly larger deviation observed in NBS glass indicates that there may be significant heterogeneity. The suggested increase in heterogeneity from K to Na to Li is, of course, consistent with the known trend in the extent of the immiscibility regions.[56] With this approach for the mixed-cation glasses, significant chemical heterogeneity is also suggested for the LN−BS and LK−BS glasses but not for the NK−BS glass, indicating that the cation mixing between Li and Na or Li and K is less homogeneous, whereas the cation mixing for K and Na is more heterogeneous.

The heterogeneity of a glass can also be monitored by the fraction of Si−O−B, which is a measure of the extent of mixing of the silicate and borate network components.[24] The fraction of Si−O−B increases in the order Li < Na < K, indicating the heterogeneity decreases in the same order, which is consistent with the NBO results. Relatively lower fractions of Si−O−B in the LN−BS and LK−BS glasses compared with those in the NBS, KBS, and NK−BS glasses are again consistent with the larger amounts of NBO in the Li-containing glasses, again indicating a higher degree of heterogeneity.

The ^{17}O chemical shift can also provide information on the type and number of cations (both network-forming and network-modifying) coordinating NBO.[29,45,46,48,57,58] In alkali borosilicate glasses, ^{11}B "wide-line" NMR has long suggested that NBO are primarily associated with Si.[9] NBO bonded to boron (denoted as B−NBO) becomes significant only at R values above $0.5 + K/4$, as monitored by the observation of "asymmetric" $^{[3]}$B.[9] Our recent ^{17}O and ^{11}B NMR studies of Li, Na, and K borosilicate glasses with high R values have confirmed this model.[59] In the composition chosen here (close to $K = 2$, $R = 0.75$), all the NBO should be Si−NBO, based both on the model and on the absence of asymmetric $^{[3]}$B from the ^{11}B MAS NMR spectra. The ^{17}O chemical shift for Si−NBO is therefore influenced mainly by the local modifier cations, which in turn is an indication of the extent of cation mixing. Values for δ_{iso} for Si−NBO, obtained from the ^{17}O 3QMAS spectra, are given in Table 4, and show clearly that in the mixed alkali glasses, the smaller cations (i.e., higher field strength) are more likely to associate with the NBO than are the larger cations, rather than being randomly mixed. For example in the LK−BS glass, δ_{iso} is close to that of the pure Li glass (43.4 versus 41.6 ppm), but far from that of the pure K glass (71.3 ppm). In contrast, the value of δ_{iso}(NBO) for the NK−BS glass is located between the values for the pure Na and K glasses, implying that Na and K both interact with NBO, although Na is slightly more competitive for this bonding environment.

In mono-alkali borosilicate glasses, ^{17}O chemical shifts of bridging oxygens are also affected by the size of the charge-balancing alkali ions.[24] Among the different types of bridging oxygens, the chemical shift for Si−O−Si is most sensitive to changes in the local structure caused by varying R and K, and is also sensitive to the type of modifier cation.[24] Isotropic peak positions for Si−O−Si in LN−BS and LK−BS (which scale directly with the chemical shift) are very similar to those in Na- and K-containing glasses, respectively (Figure 6), strongly suggesting that the cations near Si−O−Si are mainly the larger alkalis. On the other hand, there seems to be no strong preference around Si−O−Si for Na vs K in NK−BS glass since the peak position for Si−O−Si is between those of the pure Na and K glasses. It is more complicated to interpret the changes in the peaks associated with Si−O−B and B−O−B because each one is composed of two components correlated to two different boron species ($^{[3]}$B and $^{[4]}$B). For example, $^{[4]}$B−O−Si dominates in NBS and KBS, whereas in LBS the fraction of $^{[3]}$B−O−Si is slightly higher than that of $^{[4]}$B−O−Si. However, the trend from one modifier cation to another for oxygen in Si−O−B is somewhat similar to that observed for Si−O−Si.

The effects of modifier cations on ^{11}B chemical shifts are smaller than those for ^{17}O but are measurable. For example, the difference in the 3QMAS isotropic dimension $^{[3]}$B(ring) peak position between LBS and NBS/KBS is only about 1 ppm (Figure 3). It is still apparent, though, that the shifts for $^{[3]}$B(ring) in LN−BS and LK−BS are similar to those for NBS and KBS, respectively. This indicates that the modifier cations near the $^{[3]}$B-(ring) species are mostly Na or K rather than Li. The peak positions of $^{[4]}$B are complicated by varying populations of B and Si network neighbors. However, in the MAS spectra (Figure 1) the maxima for $^{[4]}$B in the Li−Na and Li−K glasses are closer to those in the NBS and KBS glasses, respectively, suggesting some preference for Na and K in these sites.

The results discussed above can be rationalized if the Li−Na and Li−K glasses undergo at least nanoscale phase separation resulting in a chemically heterogeneous intermediate-range structure, with domains close to a binary (Li-rich) alkali silicate in composition embedded in K- or Na-rich borosilicate hosts. This model

(56) Polyakova, I. G. *Phys. Chem. Glasses* **2000**, *41*, 247−258.
(57) Allwardt, J. R.; Lee, S. K.; Stebbins, J. F. *Am. Mineral.* **2003**, *88*, 949−954.
(58) Stebbins, J. F.; Oglesby, J. V.; Xu, Z. *Am. Mineral.* **1997**, *82*, 1116−1124.
(59) Du, L.-S.; Stebbins, J. F.; manuscript in preparation.

can explain the observed smaller fraction of Si−O−B and larger fraction of Si−NBO associated mainly with Li (from ^{17}O NMR), as well as the $^{[4]}$B and $^{[3]}$B(ring) species correlated mainly with Na or K (from ^{11}B NMR). In the boron-rich phase, the proximity of charged Si−O−$^{[4]}$B oxygens to Si−O−Si oxygens (because of the extensive Si/B mixing[24]) means that chemical shifts for the latter are significantly affected by the accompanying modifier or "charge balancing" alkali cations. In the Li−K and Li−Na glasses, the Si−O−Si chemical shifts thus indicate that most such oxygens interact with K or Na, consistent with the tendency of the NBO to be coordinated primarily by Li (see above), concentrated in the silica-rich phase.

In contrast to the mixed-alkali glasses containing Li, the populations and chemical shifts of oxygen and boron species in the mixed Na−K glass are very similar to the average results of NBS and KBS glasses, suggesting that Na and K cations are close to randomly mixed in these materials.

The above view of the structure of mixed alkali borosilicate glasses can be compared with previous studies of simpler systems. For example, ^{17}O DAS NMR of mixed Na−K silicate glasses showed clearly that these alkalis are distributed in random combinations around NBOs,[46] which agrees with our results for the borosilicates. Li−K and Li−Na silicate or borate glasses have not been studied in detail with ^{17}O NMR. However, in such glasses, results for ^{23}Na−^{7}Li/^{6}Li and ^{23}Na−^{23}Na dipole−dipole couplings from spin−echo double resonance (SEDOR) NMR suggested that these cations are mostly statistically mixed within a homogeneous distribution of the entire population.[35,39−42] These findings further support our contrasting interpretation that in the borosilicates the apparent strong preferences of Li vs Na/K for different coordination environments are the result of significant chemical heterogeneity, not short-range ordering. Further study of Li−Na borosilicate glasses using SEDOR and/or ^{17}O NMR studies of Li−K silicate glasses may thus be useful to determine when such heterogeneities develop.

Conclusions

High-resolution ^{11}B and ^{17}O MAS and 3QMAS spectra provide detailed information about populations of structural units and the connectivities between them in borosilicate glasses. The fractions of NBO obtained from 3QMAS spectra are generally consistent with the values derived independently from the fractions of $^{[4]}$B, indicating that the quantification of oxygen species via the 3QMAS technique (with the experimental conditions used here) is surprisingly accurate. The size of the discrepancy between the experimental values and those predicted by the Dell and Bray model[9] can further serve as an indication of the degree of chemical heterogeneity of the glasses. This increases from K- to Na- to Li-containing glasses, implying an increasing heterogeneity which is sensible in light of the increasing size of the immiscibility region from K to Na to Li borosilicates. Larger discrepancies were also found in Li−Na and Li−K mixed alkali glasses but not in Na−K glasses. Analysis of ^{17}O and ^{11}B chemical shift data suggests there are significant differences between Li and Na or K preferences for coordination by both bridging and nonbridging oxygens as well as in proximity to $^{[3]}$B and $^{[4]}$B species. In contrast, no such distinctions between Na and K are observed, implying that these cations are well-mixed. Thus, Li−Na and Li−K borosilicate glasses appear to be characterized by nanoscale heterogeneity and/or phase separation, with lithium−silicate-rich domains embedded in a sodium/potassium borosilicate host. Na−K glasses appear to be much less heterogeneous and Na and K cations are probably distributed in random combinations throughout the network.

Acknowledgment. This work was supported by the U.S. National Science Foundation (grant DMR-0100986).

CM034427R